[15] H. C. Scheer, H. Schulz, T. Hoffmann, C. M. S. Torres, *J. Vac. Sci. Technol. B* **1998**, *16*, 3917.
[16] D. Pisignano, A. Melcarne, D. Mangiullo, R. Cingolani, G. Gigli, *J. Vac. Sci. Technol. B* **2004**, *22*, 185.
[17] D. Pisignano, L. Persano, R. Cingolani, G. Gigli, *Appl. Phys. Lett.* **2004**, *84*, 1365.
[18] A. Sharma, *Langmuir* **1993**, *9*, 861.
[19] A. Faldi, R. J. Composto, K. I. Winey, *Langmuir* **1995**, *11*, 4855.
[20] X. M. Zhao, Y. Xia, G. M. Whitesides, *J. Mater. Chem.* **1997**, *7*, 1069.
[21] S. Harkema, E. Schäffer, M. D. Morariu, U. Steiner, *Langmuir* **2003**, *19*, 9714.
[22] M. Cavallini, F. Biscarini, M. Massi, A. Farran-Morales, D. A. Leigh, F. Zerbetto, *Nano Lett.* **2002**, *2*, 635.
[23] M. Cavallini, F. Biscarini, *Nano Lett.* **2003**, *3*, 1269.
[24] M. Massi, M. Cavallini, S. Stagni, A. Palazzi, F. Biscarini, *Mater. Sci. Eng., C* **2003**, *23*, 923.
[25] S. Herminghaus, A. Fery, S. Schlagowski, K. Jacobs, R. Seemann, H. Gau, W. Mönch, T. Pompe, *J. Phys.: Condens. Matter* **2000**, *12*, A57.
[26] O. Karthaus, C. Adachi, S. Kurimura, T. Oyamada, *Appl. Phys. Lett.* **2004**, *84*, 4697.
[27] T. G. Stange, D. F. Evans, W. A. Hendrickson, *Langmuir* **1997**, *13*, 4459.
[28] F. Brochard-Wyart, J. Daillant, *Can. J. Phys.* **1990**, *68*, 1084.
[29] M. Maillard, L. Motte, M. P. Pileni, *Adv. Mater.* **2001**, *13*, 200.
[30] O. Karthaus, L. Grasjo, N. Maruyama, M. Shimomura, *CHAOS* **1999**, *9*, 308.
[31] O. Karthaus, T. Koito, M. Shimomura, *Mater. Sci. Eng., C* **1999**, *8*, 523.
[32] R. D. Deegan, O. Bakajin, T. F. Dupont, G. Huber, S. R. Nagel, T. A. Witten, *Nature* **1997**, *389*, 827.
[33] J. Zhao, S. Jiang, Q. Wang, X. Liu, X. Ji, B. Jiang, *Appl. Surf. Sci.* **2004**, *236*, 131.
[34] L. M. Pismen, *Phys. Rev. E* **2004**, *70*, 021 601.
[35] X. Wang, M. Östblom, T. Johansson, O. Inganäs, *Thin Solid Films* **2004**, *449*, 125.

DOI: 10.1002/adma.200500184

Laser Scanning Lithography for Surface Micropatterning on Hydrogels**

By *Mariah S. Hahn*, *Jordan S. Miller*, and *Jennifer L. West**

Techniques that control the spatial presentation of moieties such as cell-adhesion peptides on surfaces are important for the advancement of tissue engineering, the elucidation of fundamental tissue structure–function relationships, and the formation of immobilized cell and protein arrays for biotechnology.[1] Cell and protein patterns have previously been created using a range of methods, including photolithography[2,3] and soft-lithographic approaches such as microcontact printing,[4] microfluidic patterning,[5,6] and micromolding.[7,8] The patterned substrates have generally been modified silicon or glass,[9,10] whereas surface patterning of deformable, solvated substrates has not received a similar degree of attention. Many commonly used patterning techniques cannot be readily applied to high-fidelity patterning of deformable, solvated substrates. For example, microcontact printing is generally not applicable to such substrates due to lateral diffusion of the patterned molecule when the inked stamp comes into contact with the solvated substrate. Given the importance of deformable, solvated substrates, such as hydrogels, as scaffolds for soft tissue engineering applications, development of methods for direct, high-fidelity surface patterning of these substrates is desirable. This work develops confocal-based laser scanning lithography (LSL)[11,12] for two-dimensional (2D) and three-dimensional (3D) surface patterning of hydrated, photoactive poly(ethylene glycol) (PEG)-based hydrogel substrates.

PEG-based hydrogels are biocompatible and intrinsically resistant to protein adsorption and cell adhesion, thus providing a biological "blank slate" upon which desired biofunctionality can be built.[13] Acrylate-terminated PEG macromers undergo rapid polymerization upon exposure to UV or visible light when in the presence of appropriate photoinitiators.[14,15] In this work, confocal-based LSL is used to surface pattern photoactive PEG-diacrylate (PEGDA) hydrogel substrates according to the methodology shown schematically in Figure 1. Briefly, a preswelled PEGDA hydrogel is positioned on the stage of a confocal laser scanning microscope (LSM), which is focused on the upper surface of the substrate. The user then creates a "virtual mask" by drawing "regions of interest" (ROIs), i.e., regions where laser irradiation is desired, using standard confocal LSM software. The LSM software converts these ROIs into instructions that dictate at which pixel locations the laser shutter is opened during an irradiation cycle. A thin layer of precursor solution containing fluorescently labeled acryloyl-PEG-peptide (ACRL-PEG-peptide) and a photoinitiator is then spread onto the substrate surface. Patterning is carried out using an irradiation cycle in which a laser line (selected to match the photoinitiator absorption band) is unidirectionally scanned across the ROIs at user-defined exposure times and intensity. Pattern arrays can be formed using a programmable motorized stage and sequential irradiation cycles. Unbound ACRL-PEG-peptide is rinsed away with phosphate-buffered saline (PBS), and the patterned regions can be observed via fluorescence microscopy.

Since the PEGDA hydrogels are swelled prior to surface patterning, feature distortion due to substrate swelling post-patterning is not an issue. Thus, a wide range of features, including free-form objects (Fig. 2a) and patterns down to at least 5 μm in size (Fig. 1), can be generated with high fidelity on the hydrated gel surfaces using this procedure. Since the

[*] Dr. J. L. West, Dr. M. S. Hahn, J. S. Miller
Department of Bioengineering
Rice University
MS 144, 6100 Main Street, Houston, TX 77005 (USA)
E-mail: jwest@rice.edu

[**] The authors acknowledge the NIH and the NSF for funding this work.

ADVANCED MATERIALS

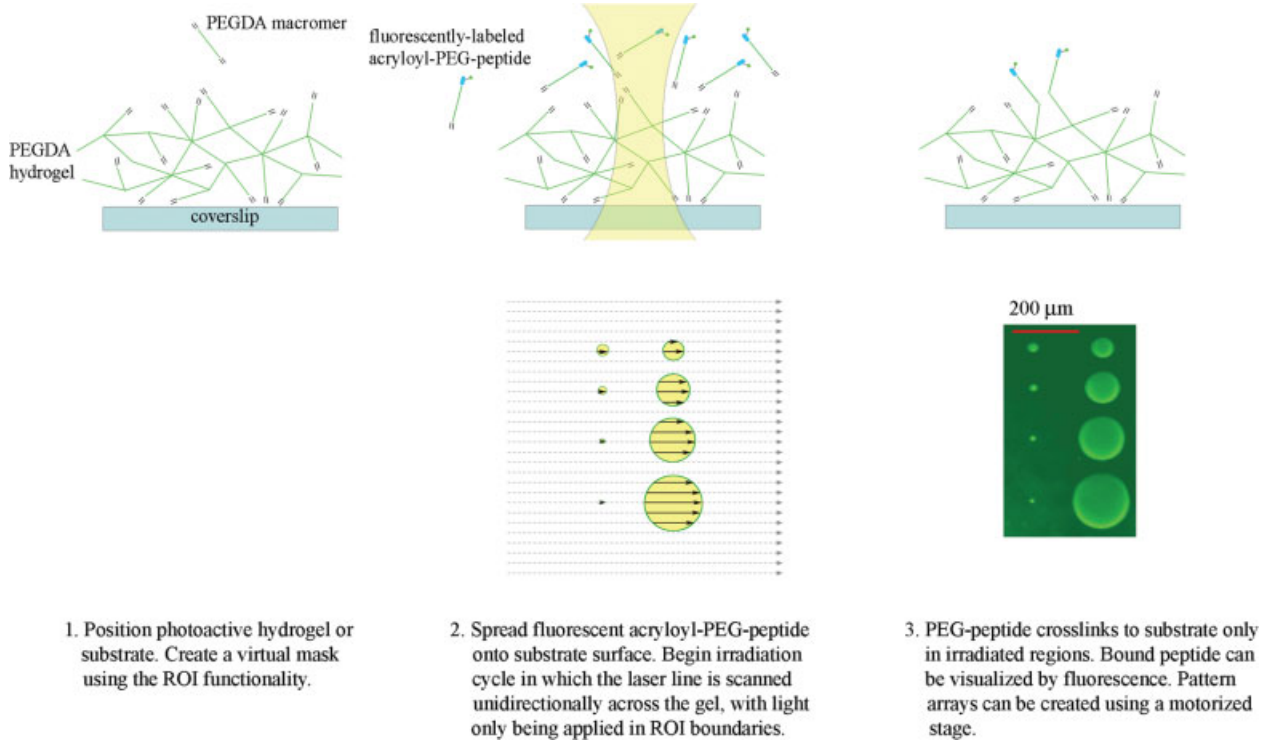

Figure 1. Schematic of surface patterning of photoactive substrates using LSL, with PEGDA hydrogels used as the model substrate. The upper row of images illustrates the patterning mechanism at the molecular level, transverse to the plane of the substrate surface. The bottom row of images depicts the patterning methodology at the macroscopic level, parallel to the substrate surface. The fluorescence image in the lower right-hand corner is of an actual hydrogel surface patterned with fluorescent ACRL-PEG-RGDS and demonstrates that features down to ~5 µm in size can be produced. ROI: region of interest; ACRL: acryloyl; RGDS: arginine–glycine–aspartic acid–serine.

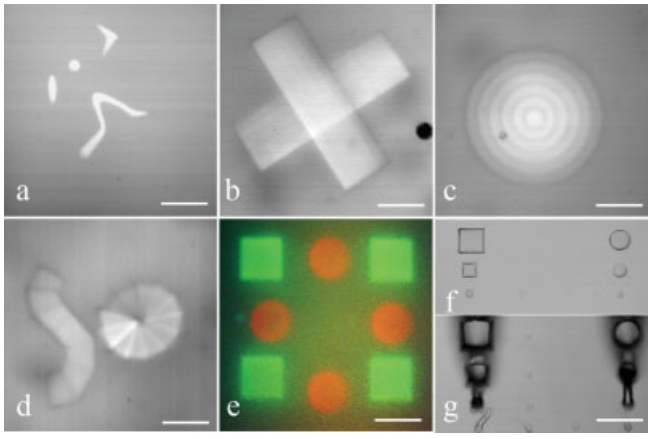

Figure 2. Demonstration of the versatility of LSL hydrogel surface patterning. a) A grayscale fluorescence image of free-form ROIs patterned with fluorescently labeled ACRL-PEG-RGDS. b–d) Grayscale fluorescence images of 2D concentration gradients of ACRL-PEG-RGDS formed by varying irradiation exposure times across ROIs. Note the flexibility in orientation of the patterned regions. e) A fluorescence image of a PEGDA hydrogel patterned with two different adhesive peptides (ACRL-PEG-RGDS in green and ACRL-PEG-REDV (REDV: arginine–glutamic acid–aspartic acid–tyrosine) in red). f,g) Differential interference contrast images of 3D patterns formed by including PEGDA in the precursor solution. Features in (f) are ~4 µm in height, while those in (g) are ~20 µm in height. Note the axial variation in feature size in (g) due to laser beam diffraction from its focal point. Scale bars = 200 µm.

surface density of bound ACRL-PEG-peptide in the irradiated ROIs is dependent on user-specified irradiation exposure time and intensity, the surface peptide concentration can be spatially controlled by the user, allowing for complex 2D concentration gradients to be formed (Figs. 2b–d). This level of spatial control over irradiation exposure is not readily achieved using conventional photolithographic masks. In fact, surface-concentration gradients created using standard photolithography generally result from spatially varying the spacing between patterned stripes of uniform concentration rather than from varying the density of bound molecule within the patterned regions.[16,17] By incorporating intermediate wash steps between sequential irradiation cycles, multiple bioactive peptides can be patterned onto the hydrogel surface (Fig. 2e). If cell-specific adhesive peptides are used, multiple cell types could be specifically attached to different regions of the substrate, permitting the creation of spatially defined multicellular arrays and co-cultures.

As shown schematically in Figure 1, monolayer surface patterns are created when the precursor solution contains only monoacrylate-derivatized PEG-peptides. This feature should permit the effects of the peptide concentration and feature 2D geometry on cell behavior to be studied independently of the effects of topography. However, since confocal irradiation is not limited to the laser beam focal plane, irradiation can result in 3D surface patterns if diacrylate-derivatized PEG

macromers are added to the precursor solution (Figs. 2f,g). Features ranging from 0 to roughly 5 μm in height can be formed with low axial distortion (Fig. 2f), although the fidelity of the patterned features is reduced as the thickness of the precursor solution layer increases due to laser beam diffraction from its focal point (features are ~4 μm height in Fig. 2f versus ~20 μm height in Fig. 2g). 3D microstructures have been used to provide topographical cues to control cellular organization.[18,19] By combining ACRL-PEG-peptides with PEGDA to form various 3D structures on hydrogel surfaces, the combined effects of pattern topography and peptide concentration on cell behavior can be explored.

To evaluate the feasibility of using LSL-patterned PEGDA hydrogels for spatially controlled cell attachment, human dermal fibroblasts (HDFs) were seeded onto monolayer patterns of ACRL-PEG-RGDS. As expected, cells selectively adhered to hydrogel regions patterned with the cell-adhesive peptide RGDS (Fig. 3). When HDFs were seeded on a spiral RGDS gradient pattern generated by revolving a triangular ROI through 360° and doubling exposure time with each 30° rotation, the cells aligned in the direction of the gradient (Fig. 3d). Concentration gradients of ligands such as RGDS,[20] heparin,[16] laminin,[21] and certain growth factors[17,20] have been shown to control the alignment, growth, and locomotion of a variety of cell types, and thus these gradients can be used to guide cell behavior. Since cell behavior and morphology are also heavily influenced by pattern geometry,[22] confocal LSL can be used to study the interplay of geometrical constraints and moiety-concentration gradients on cell behavior.

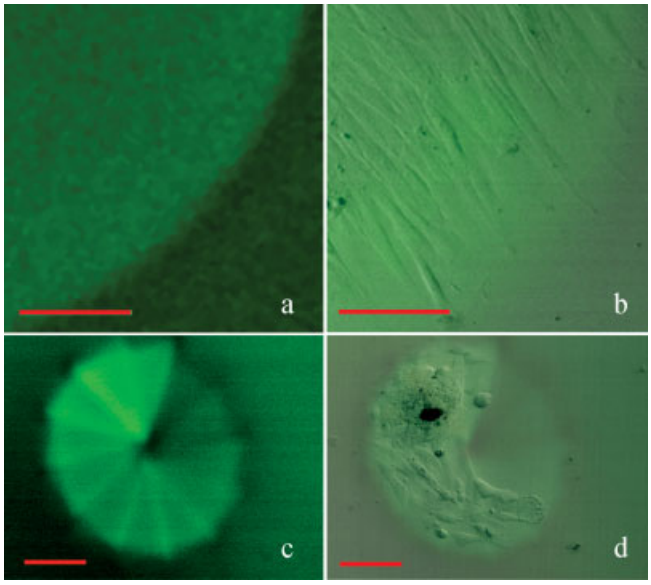

Figure 3. Cell adhesion on LSL-patterned PEGDA hydrogel substrates. a) Fluorescence image of an ACRL-PEG-RGDS surface pattern. b) Differential interference contrast (DIC) image of a confluent HDF monolayer overlaid onto the corresponding fluorescence pattern image in (a). Note that the HDFs are localized within the boundaries of the ACRL-PEG-RGDS patterned region. c) Fluorescence image of a spiral concentration gradient pattern of ACRL-PEG-RGDS. d) DIC image of adherent HDFs overlaid onto the corresponding fluorescence pattern image in (c). Note that the cells are localized within the patterned region and have elongated in the direction of the gradient. The effects of reduced RGDS levels on cell adhesion are also demonstrated in this image. Scale bars = 100 μm.

In conclusion, a versatile confocal-based laser scanning lithographic method for controlled, high-fidelity 2D and 3D surface patterning of PEGDA hydrogels has been presented. Although PEGDA hydrogels have been used as model substrates to demonstrate LSL patterning, this method can be applied to any optically clear, photoactive substrate, whether rigid or deformable. LSL employs user-defined "virtual masks" to spatially control laser irradiation during pattern generation, eliminating the need for conventional photolithographic masks and a clean room. Moreover, patterned biomolecules are covalently immobilized onto the substrate surface, resulting in mechanically and chemically stable patterns. In the present work, the surface properties of deformable, biocompatible PEGDA hydrogels have been modified in a controlled manner using LSL, with pattern feature sizes down to at least 5 μm being achievable. HDFs have been shown to selectively bind to regions patterned with appropriate cell-adhesive peptides and to retain their spatial localization in culture. Complex 2D concentration gradients of patterned peptides have been generated via user alteration of irradiation exposure levels across ROIs. 3D surface structures with heights under ~5 μm have also been created with high fidelity by incorporating PEGDA macromers into the precursor solution. Since both 2D and 3D surface patterns can be formed, LSL should allow for the controlled study of the separate effects of pattern 2D geometry versus pattern topography on cell behavior. The flexibility offered by this technique in terms of feature topography, bound peptide concentration, and substrate type is particularly desirable in tissue engineering applications, where patterning often seeks to mimic the complex organization of soft tissues. Controlled functionalization of surfaces should allow for increased insight into cell behavior, cell–cell interactions, and cell–biomaterial interactions and for the elucidation of fundamental structure–function relationships of tissues.

Experimental

Cell Maintenance: HDFs (Cambrex) were maintained in Dulbecco's Modified Eagle Medium (DMEM) supplemented with 10 % Fetal Bovine Serum (FBS), 2 mM L-glutamine, 100 U mL^{-1} penicillin, and 100 mg L^{-1} streptomycin at 37 °C/5 % CO_2. Cells were used at passages 7–12. All cell-culture reagents were obtained from Sigma.

Polymer Synthesis: PEGDA with a molecular weight (MW) of 3400 g mol^{-1} was prepared by combining 0.1 mmol mL^{-1} dry PEG (MW 3400 g mol^{-1}, Fluka), 0.4 mmol mL^{-1} acryloyl chloride, and 0.2 mmol mL^{-1} triethylamine in anhydrous dichloromethane (DCM) and stirring under argon overnight. The resulting solution was washed with 2 M K_2CO_3 and separated into aqueous and DCM phases to remove HCl. The DCM phase was subsequently dried with anhydrous $MgSO_4$, and PEGDA was precipitated in diethyl ether, filtered, and dried under vacuum.

ADVANCED MATERIALS

Fluorescently Labeled PEG-Peptide Synthesis: Peptides RGDS (American Peptide) and REDV (American Peptide) were conjugated to PEG (MW 3400 g mol^{-1}) by reaction with ACRL-PEG-NHS (Nektar, NHS: *N*-hydroxysuccinimide) in a 1:1 molar ratio for 2 h in 50 mM sodium bicarbonate buffer, pH 8.5. Alexa Fluor 488 carboxylic acid, tetrafluorophenyl (TFP) ester (Molecular Probes) was then added to the ACRL-PEG-RGDS reaction mixture at approximately 10 moles dye per mole PEG-peptide and allowed to react for 1 h at room temperature. Alexa Fluor 594 carboxylic acid, TFP ester (Molecular Probes) was similarly added to the ACRL-PEG-REDV and allowed to react for 1 h at room temperature. The desired products were purified by dialysis and then lyophilized.

Photopolymerization of PEGDA Hydrogels: A solution was prepared containing 10 % (w/v) PEGDA and 1.5 % (v/v) triethanolamine (TEOA) in *N*-(2-hydroxylethyl)piperazine-*N*′-(2-ethanesulfonic acid) (HEPES)-buffered saline (pH 7.4, HBS), 0.4 % (v/v) *N*-vinylpyrrolidone (NVP), and 100 μM eosin Y (a biocompatible, visible-light photoinitiator). This solution was polymerized between two glass plates separated by 0.5 mm spacers by exposure to white light.

Laser Scanning Lithography: The surface of a pre-swelled PEGDA hydrogel was positioned at the focal plane of a 10× Plan-Apochromat objective (numerical aperture (*NA*) 0.45) attached to a LSM 510 META confocal microscope (Zeiss). Virtual masks were drawn using the ROI function of the LSM software.

Two-Dimensional Surface Patterns: A thin layer of fluorescently labeled ACRL-PEG-peptide (30 μmol mL^{-1}) dissolved in HBS/TEOA containing 0.4 % NVP and 100 μM eosin Y was spread onto the surface of the PEGDA gel. For the fluorescence pattern images in Figures 1,2a,3, patterning was carried out using an irradiation cycle in which a 514 nm argon ion laser line was unidirectionally scanned across the specified ROIs at 0.30 mW μm^{-2} and 60 μs μm^{-2}. Unbound ACRL-PEG-peptide was rinsed away with sterile PBS. For the gradient patterns in Figures 2b–d, 514 nm argon ion laser power was maintained at 0.30 mW μm^{-2}; however, a range of irradiation times were used across ROIs, with a minimum exposure time of 0.5 μs μm^{-2}. Successful patterning of the fluorescently labeled peptides was confirmed by visualization under fluorescence (Zeiss LSM 510 META). The bioactivity of patterned cell adhesion peptide RGDS was evaluated by seeding HDFs onto patterned hydrogel surfaces and examining cell adhesion via DIC imaging (Zeiss LSM 510 META) at days 1 and 4.

Three-Dimensional Surface Patterns: A thin layer of 0.2 g mL^{-1} MW 600 g mol^{-1} PEGDA (Sarcomer) dissolved in HBS/TEOA containing 0.4 % NVP and 100 μM eosin Y was spread onto the surface of the PEGDA gel. Patterning was carried out using an irradiation cycle in which a 514 nm argon ion laser line was unidirectionally scanned across the specified ROIs at 0.30 mW μm^{-2} and 60 μs μm^{-2}. Unbound ACRL-PEG-peptide was rinsed away with sterile PBS, and patterning was confirmed through DIC imaging (Zeiss LSM 510 META).

Received: January 26, 2005
Final version: August 13, 2005
Published online: November 5, 2005

[1] T. Chovan, A. Guttman, *Trends Biotechnol.* **2002**, *20*, 116.
[2] D. Ryan, B. A. Parviz, V. Linder, V. Semetey, S. K. Sia, J. Su, M. Mrksich, G. M. Whitesides, *Langmuir* **2004**, *20*, 9080.
[3] C. B. Herbert, T. L. McLernon, C. L. Hypolite, D. N. Adams, L. Pikus, C.-C. Huang, G. B. Fields, P. C. Letourneau, M. D. Distefano, W.-S. Hu, *Chem. Biol.* **1997**, *4*, 731.
[4] C. S. Chen, M. Mrksich, S. Huang, G. M. Whitesides, D. E. Ingber, *Biotechnol. Prog.* **1998**, *14*, 356.
[5] S. Takayama, J. C. McDonald, E. Ostuni, M. N. Liang, P. J. A. Kenis, R. F. Ismagilov, G. M. Whitesides, *Proc. Natl. Acad. Sci. USA* **1999**, *96*, 5545.
[6] E. Delamarche, A. Bernard, H. Schmid, B. Michel, H. Biebuyck, *Science* **1997**, *276*, 779.
[7] K. Y. Suh, J. Seong, A. Khademhosseini, P. E. Laibinis, R. Langer, *Biomaterials* **2004**, *25*, 557.
[8] A. Khademhosseini, S. Jon, K. Y. Suh, T.-N. T. Tran, G. Eng, J. Yeh, J. Seong, R. Langer, *Adv. Mater.* **2003**, *15*, 1995.
[9] Y. Xia, G. M. Whitesides, *Angew. Chem. Int. Ed.* **1998**, *37*, 550.
[10] R. S. Kane, S. Takayama, E. Ostuni, D. E. Ingber, G. M. Whitesides, *Biomaterials* **1999**, *20*, 2363.
[11] C. Rensch, S. Hell, M. V. Schickfus, S. Hunklinger, *Appl. Opt.* **1989**, *28*, 3754.
[12] L. P. Ghislain, V. B. Elings, K. B. Crozier, S. R. Manalis, S. C. Minne, K. Wilder, G. S. Kino, C. F. Quate, *Appl. Phys. Lett.* **1999**, *74*, 501.
[13] W. R. Gombotz, G. H. Wang, T. A. Horbett, A. S. Hoffman, *J. Biomed. Mater. Res.* **1991**, *25*, 1547.
[14] J. L. West, J. A. Hubbell, *React. Polym.* **1995**, *25*, 139.
[15] J. L. Hill-West, S. M. Chowdhury, M. J. Slepian, J. A. Hubbell, *Proc. Natl. Acad. Sci. USA* **1994**, *91*, 5967.
[16] Y. Ito, M. Hayashi, Y. Imanishi, *J. Biomater. Sci., Polym. Ed.* **2001**, *12*, 367.
[17] G. Chen, Y. Ito, *Biomaterials* **2001**, *22*, 2453.
[18] S. Sarkar, M. Dadhania, P. Rourke, T. A. Desai, J. Y. Wong, *Acta Biomaterialia* **2005**, *1*, 93.
[19] R. G. Flemming, C. J. Murphy, G. A. Abrams, S. L. Goodman, P. F. Nealey, *Biomaterials* **1999**, *20*, 573.
[20] S. A. DeLong, J. J. Moon, J. L. West, *Biomaterials* **2005**, *26*, 3227.
[21] S. K. Dertinger, X. Jiang, Z. Li, V. N. Murthy, G. M. Whitesides, *Proc. Natl. Acad. Sci. USA* **2002**, *99*, 12 542.
[22] A. Brock, E. Chang, C. C. Ho, P. LeDuc, X. Jiang, G. M. Whitesides, D. E. Ingber, *Langmuir* **2003**, *19*, 1611.

DOI: 10.1002/adma.200501660

Disorder-Induced Optical Heterogeneity in Single CdSe Nanowires**

By *Vladimir V. Protasenko*, *Katherine L. Hull*, and *Masaru Kuno**

The optical, electrical, and transport properties of semiconductor nanowires (NWs) differ significantly from those of quantum dots (QDs) or quantum wells. Namely, the two-dimensional (2D) confinement of carriers in NWs leaves one degree of freedom enabling high carrier mobilities, a natural resistance to scattering, and intrinsic polarization anisotropy in absorption and emission. Quantization effects also increase

[*] Prof. M. Kuno, V. V. Protasenko, K. L. Hull
Department of Chemistry and Biochemistry
Notre Dame Radiation Laboratory, University of Notre Dame
251 Nieuwland Science Hall, Notre Dame, IN 46556 (USA)
E-mail: mkuno@nd.edu

[**] We thank V. S. Dneprovskii, E. A. Muljarov, and Al. L. Efros for helpful discussions. This work was supported by the ACS Petroleum Research Fund, the Notre Dame Faculty Research Program, and by the University of Notre Dame. We thank the Notre Dame Radiation Laboratory and the Office of Basic Energy Sciences of the U.S. Department of Energy for use of their facilities. Supporting Information is available online from Wiley InterScience or from the author.